Supporting Information

Augmenting Second Harmonic Generation using Fano Resonances in Plasmonic Systems

Krishnan Thyagarajan, Jérémy Butet, and Olivier J. F. Martin

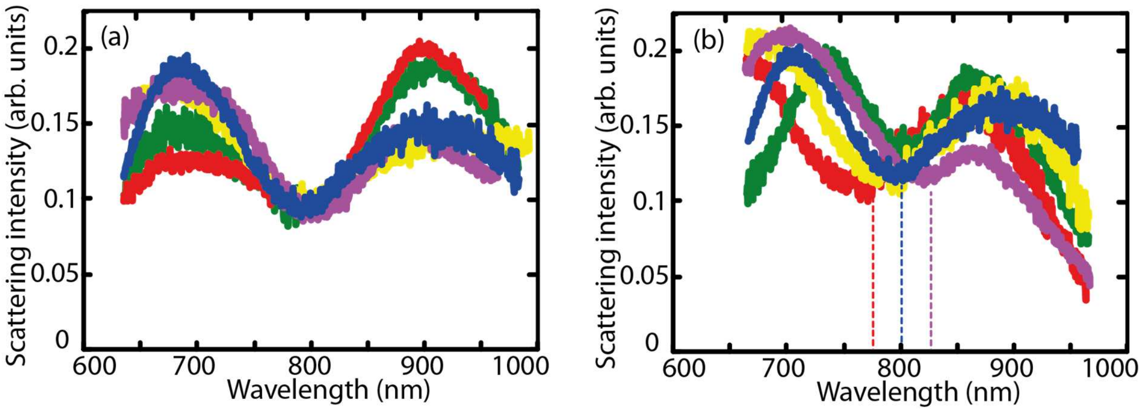

Figure S1: Linear optical scattering spectra measured (a) for five different silver heptamers from the array showing good agreement of the spectral features with the designed structure including a Fano dip at around λ=800 nm and (b) for some heptamers located at the edges of the array showing variation in the position of the dip, perhaps caused by a non-perfect lift-off. This indicates that any randomly selected structures from the array exhibit the required characteristics, although there are some structures at the edges of the array which deviate from the expected features. This causes an overall inhomogeneous broadening of the linear response, which also affects the SHG efficiency.

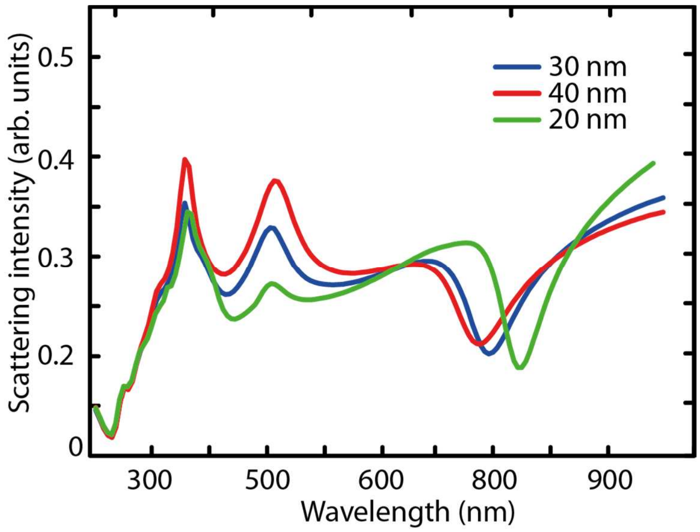

Figure S2: Calculated scattering spectra for different silver heptamers with same dimensions as in Fig. 1, but three different gaps: 20, 30 and 40 nm. These structures reproduce well the inhomogeneous broadening observed for the experimental structures shown in Fig. S1b. The shift in the position of the Fano dip has an effect on the scattering efficiency at the second harmonic, as illustrated in Fig. S3.

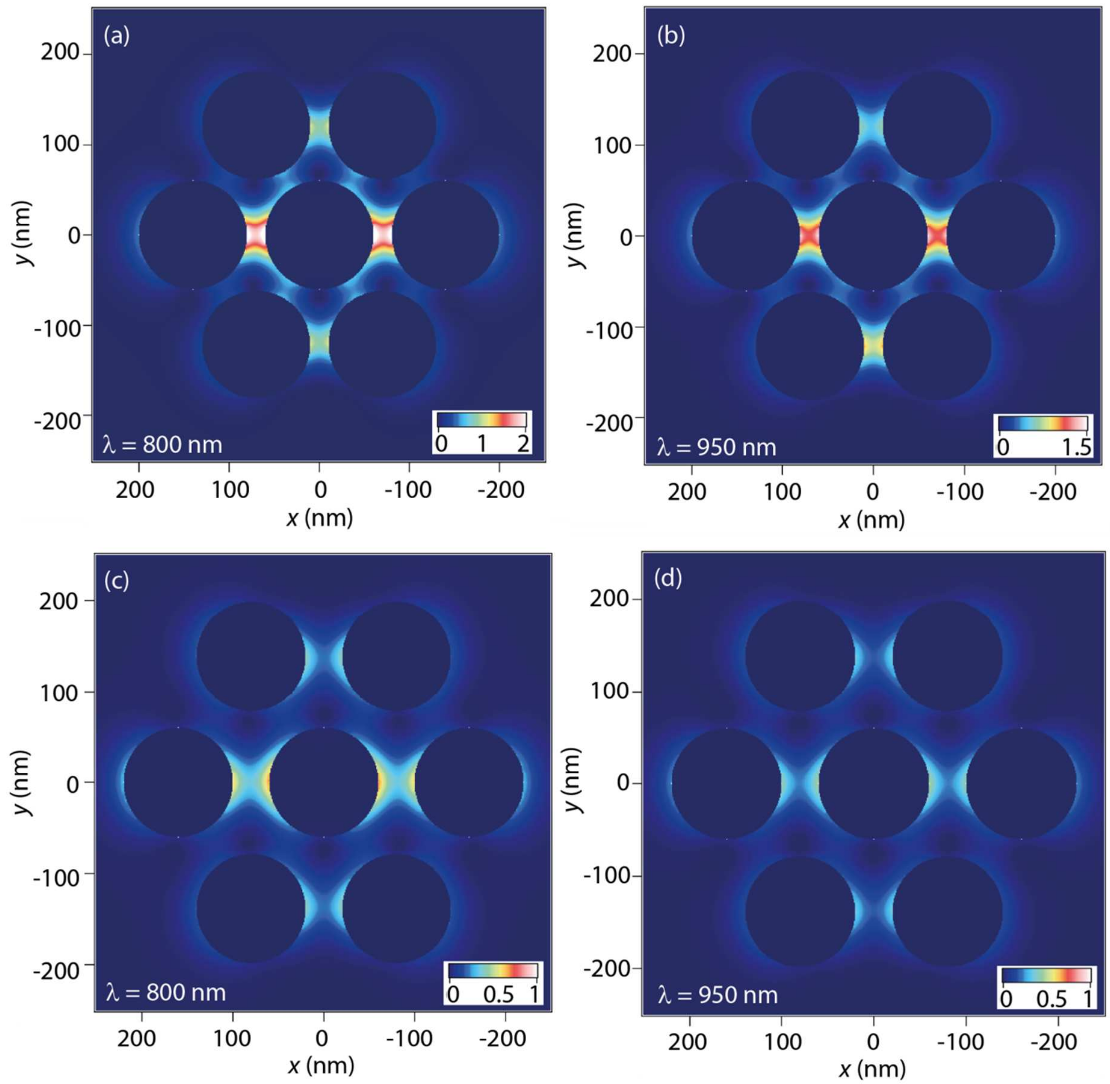

Figure S3: Near-field intensity enhancement distribution of the fundamental intensity shown on a normalized linear scale for the same silver heptamer with a 20 nm gap at (a) λ=800 nm and (b) λ=950 nm incidence wavelength, and for a 40 nm gap at (c) λ=800 nm and (d) λ=950 nm incidence wavelength.

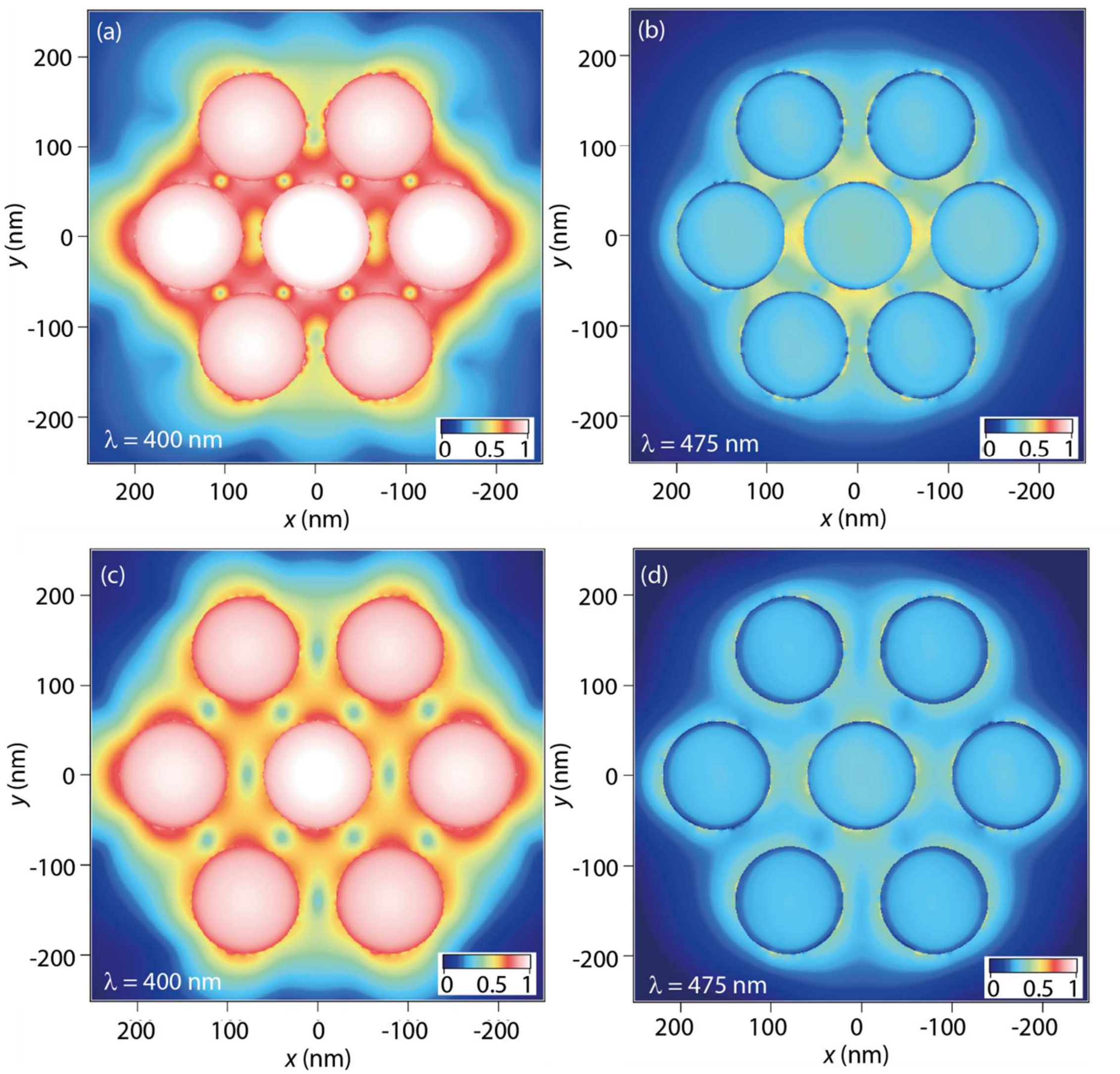

Figure S4: Near-field intensity enhancement distribution of the SHG intensity shown on a normalized logarithm scale for the same silver heptamer with a 20 nm gap at (a) λ=400 nm and (b) λ=475 nm (λ=800 nm and λ=950 nm incidence wavelength, respectively), and for a 40 nm gap at (c) λ=400 nm and (d) λ=475 nm (λ=800 nm and λ=950 nm incidence wavelength, respectively).

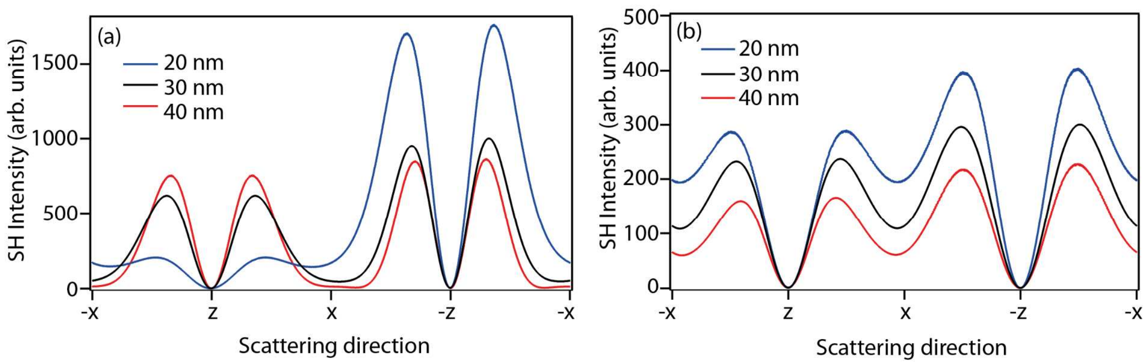

Figure S5: SH intensity scattered along different directions at (a) λ= 400 nm (incidence fundamental wavelength λ= 800 nm) and (b) λ= 475 nm (incidence fundamental wavelength λ= 950 nm) for the three different gaps studied in Fig. S2.

Discussion:

Due to fabrication imperfections, the gaps between the different particles within a heptamer may vary, as can be seen from the experimental curves in Fig. S1. These imperfections may cause the Fano resonance dip to differ from the designed λ= 800 nm position. The curves in Fig. S1a show that most of the heptamers exhibit the targeted scattering features, however, Fig. S1b indicates that some of the structures exhibit dips shifted between λ= 775 nm and λ= 825 nm. We have calculated that structures with gaps of 20 nm and 40 nm instead of 30 nm, can be used to model these features, as shown in Fig. S2. To show that this fabrication inhomogeneity affects the field localization at the fundamental wavelength for incidence wavelengths of λ= 800 nm and λ= 950 nm, the corresponding near-field plots are shown in Fig. S3. The 20 nm gap structures exhibit a larger field enhancement than the designed 30 nm gap structures, while the 40 nm gap structures show weaker enhancement at the fundamental wavelength. To investigate the corresponding impact on the SHG, the near-field plot at λ=400 nm and λ=475 nm, corresponding to a fundamental excitation at λ=800 nm and λ=950 nm respectively, are shown in Fig. S4 and indicate that the near-field at the second harmonic is also affected by the inhomogeneity. This is emphasized in Fig. S5, where it is seen that changing the gap from 30 nm to 20 nm decreases the SH intensity from 600 to 200 for a fundamental wavelength λ=800 nm, while it increases from 210 to about 290 in the collection direction for a fundamental wavelength λ=950 nm. In conclusion, fabrication inhomogeneities can explain that the experimental SHG augmentation reaches only 1.5, while the theoretically predicted value was 3 times.